Available online at www.sciencedirect.com
ScienceDirect
Polymer 48 (2007) 7567–7572
polymer
www.elsevier.com/locate/polymer

Structure–properties relationships in clay nanocomposites based on PVDF/(ethylene–vinyl acetate) copolymer blends

Antonios Kelarakis [a,*], Emmanouel P. Giannelis [a], Kyunghwan Yoon [b]

[a] *Department of Materials Science and Engineering, Cornell University, Ithaca, NY 14853, USA*
[b] *Department of Chemistry, Stony Brook University, Stony Brook, NY 11794-3400, USA*

Received 29 June 2007; received in revised form 28 October 2007; accepted 3 November 2007
Available online 7 November 2007

Abstract

The relationships between the microscopic structure and the macroscopic properties in two sets of clay nanocomposites based on polymer blends comprised of poly(vinylidene fluoride) (PVDF) and ethylene–vinyl acetate copolymer (EVAc) were examined. In nanocomposites based on a polymer blend matrix with high content of polar groups (VAc) the dispersion of polar nanoclay leads to significant enhancement in toughness and a substantial increase in viscosity. However, in nanocomposite blends based on a less polar matrix (i.e. with fewer VAc groups) it is the hydrophobic organoclay that leads to higher modulus and stronger viscoelasticity. The dispersion of nanoparticles and the mechanical response are discussed in terms of emulsifying efficiency of the clay particles in the immiscible polymer blend, an effect that largely depends on the localized interactions between the polymer groups and the clay surface modifier. The potential of nanoclays to serve as matrix sensitive structure-directing agents in tailor-made materials is demonstrated.

Keywords: Nanocomposite; Blend; Nanoclay

1. Introduction

One of the most prominent challenges in nanocomposites [1–4] is to understand and ultimately control the interfacial structure and dynamics. The interfacial structure and dynamics are governed by the type of interactions present between the polymer matrix and the embedded nanoparticles. These interactions have a critical effect on the macroscopic properties of the nanocomposites, and can be dramatically altered by properly controlling the surface chemistry of the nanoparticles and/or the type of bonding between the polymer and the nanoparticles. In the case of clay nanoparticles, surface modification can be readily accomplished using a simple cation-exchange reaction to replace the native cations in the pristine clay with ammonium ions. Depending on the choice of the ammonium ion used the ion-exchange can essentially reverse the hydrophilic character of the clay to a hydrophobic one and can, therefore, enable sufficient dispersion of the clay particles into a wide range of polymer matrices. The final dispersion in the nanocomposites reflects the silicate–silicate, polymer–polymer and silicate–polymer interactions, which in turn, are largely governed by the nature of the ammonium ion used for surface modification of the clay nanoparticles and the type of polymer.

Despite the considerable body of work in organic–inorganic hybrids, relatively limited information is available regarding nanocomposites based on polymer blends. Nevertheless, the emulsifying efficiency of the silicate nanoparticles to miscible [5] and immiscible [6–16] blends has been well documented.

In the present study we focus on poly(vinylidene fluoride) (PVDF)/ethylene–vinyl acetate (EVAc) blends because incorporation of nanoclay into PVDF was shown to have a remarkable effect on crystal development of the polymer and the mechanical response of the resulting nanocomposites [17–19]. Two different copolymers with various percentages of VAc groups were

* Corresponding author.
E-mail address: akelar@cc.uoa.gr (A. Kelarakis).

0032-3861/$ - see front matter © 2007 Elsevier Ltd. All rights reserved.
doi:10.1016/j.polymer.2007.11.005

used. Increasing the VAc content of the copolymer leads to an increase in the density of polar groups and, in that sense, the use of EVAc copolymers offers the possibility of altering the matrix by simply varying the relative portions of the two monomers in the copolymer. For the nanocomposite blends two different, commercially available organically modified clays were used. One, Cloisite 30B, is ion exchanged with a polar ammonium ion while the other, I.30T is based on nonpolar modifiers.

2. Experimental section

2.1. Preparation of the nanocomposites

Powdered poly(vinylidene fluoride) was kindly supplied by Atofina Chemical Co. (resin grade PVDF, Kynar 721). The two ethylene–vinyl acetate (EVAc) random copolymers, namely Elvax® 150 (32 wt.% VAc, m.p. 63 °C) and Elvax® 560 (15 wt.% VAc, m.p. 92 °C) were provided by DuPont Packaging and Industrial Polymers. Each one of these copolymers was blended separately with PVDF; PVDF/EVAc32 and PVDF/EVAc15 refer to blends with Elvax® 150 and Elvax® 560, respectively. Two commercial organically modified montmorillonite clays were used; Cloisite 30B from Southern Clay Products is a bis(hydroxyethyl)methyl tallow ammonium-exchanged montmorillonite. I.30T from Nanocor Inc. is also a montmorillonite and is ion exchanged octadecyltrimethyl ammonium ions. Both of the clays used are quaternary ammonium compounds; the presence of two hydroxyl groups give polar characteristic to Cloisite 30B, while clay I.30T is typically hydrophobic.

Prior to nanocomposites preparation, all materials were dried in a vacuum oven overnight. PVDF/EVAc 70:30 blends were used. All nanocomposites contained 5 wt.% clay. The components were first thoroughly mixed in a Flack-Tek DAC-150 FV speed mixer, before being melt coextruded with a twin screw at 200 °C under nitrogen flow (for 5 min). Specimens of suitable shape (dumbbell for Instron tests, rings for rheology) and size were prepared by a Daca Instruments microinjector with the barrel at 220 °C, the mold at room temperature and the injection pressure at 100 psi.

2.2. Methods

Wide-angle, X-ray diffraction (WAXS) spectra were recorded at room temperature using a Scintag Inc. $\theta-\theta$ difractometer (Cu Kα radiation, $\lambda = 1.54$ Å). Differential scanning calorimetry was performed on a TA Instrument Q1000 series calorimeter over the temperature range 10–200 °C at a scan rate of 10 °C/min. Morphologies of cryogenically fractured samples were studied using a Leo 1550 microscope operated at an acceleration voltage of 10 kV. All samples were gold coated in order to reduce charge effects.

Tensile tests were performed at room temperature with an Instron 5500 Mechanical Tester at constant strain rate of 5 mm/min following standard ASM protocols. Rheological properties were determined using a Paar Physica Modular Compact Rheometer 300 (MCR 300) equipped with parallel plate geometry (diameter 25 mm). Measurements were performed in small amplitude oscillatory shear, at a fixed temperature of 210 °C, in a dry nitrogen atmosphere to suppress oxidative degradation. The samples were kept for 30 min in the rheometer for thermal equilibration and structural relaxation, before any measurements were performed.

3. Results and discussion

XRD patterns of the nanocomposite samples are shown in Fig. 1a and b. The patterns of the neat nanoclays are also included for comparison. The expansion of the interlayer galleries of the clay particles in the composites compared to the basal spacing of the neat clays is indicative of intercalated hybrids. However, only the PVDF/EVAc32–I.30T nanocomposite shows a well-ordered intercalated structure. The PVDF/EVAc15–30B nanocomposite as well as both nanocomposite blends based on 30B show more disordered structures. The difference in order/dispersion reflects differences in the hydrophilicity/hydrophobicity of the two polymer blends and the corresponding nanoparticles. The XRD spectra at higher angles are shown in Fig. 2. The crystalline peaks observed

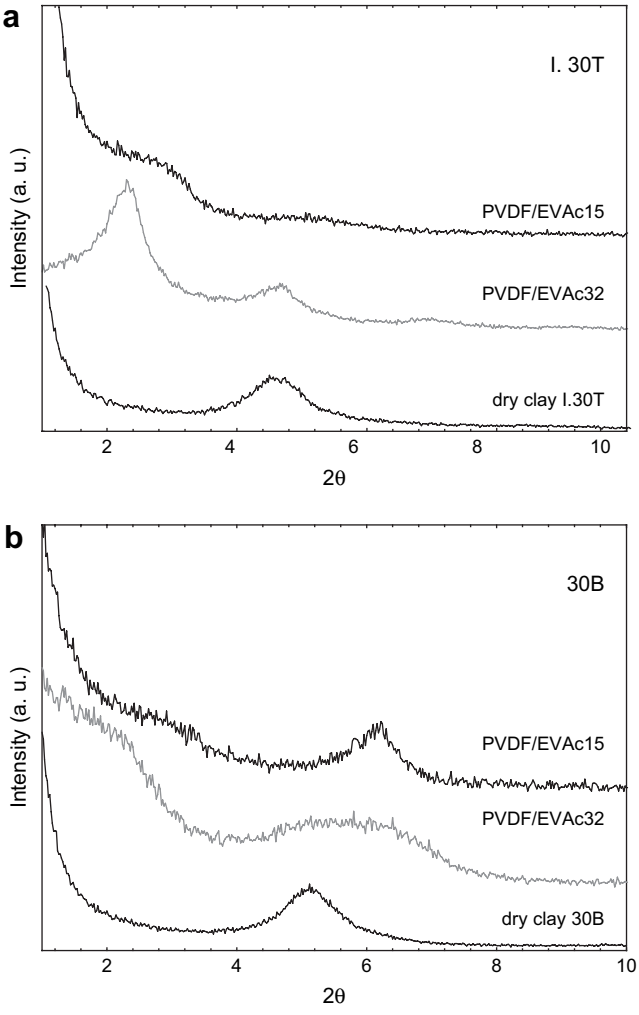

Fig. 1. XRD patterns of the nanocomposites and the corresponding clay nanoparticles: (a) clay I.30T and (b) clay 30B.

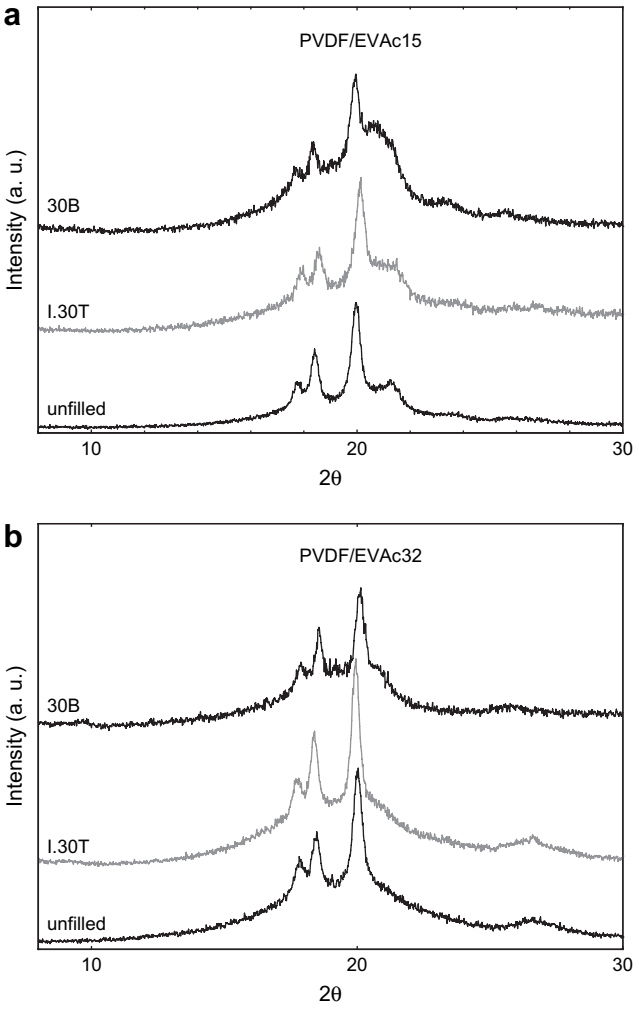

Fig. 2. XRD patterns of the unfilled blends and the corresponding nanocomposites: (a) PVDF/EVAc15 system and (b) PVDF/EVAc32 system.

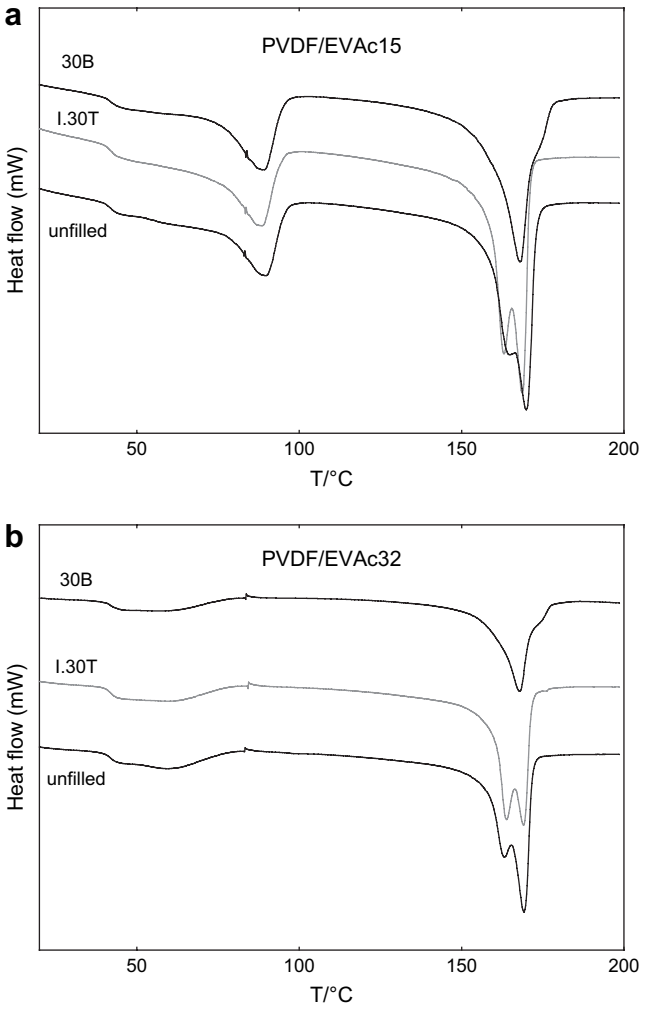

Fig. 3. DSC thermographs of the unfilled samples and the corresponding ternary systems: (a) PVDF/EVAc15 system and (b) PVDF/EVAc32 system.

for the unfilled blends can be indexed [20] as the reflection peaks of the α-phase of PVDF. Addition of clay nanoparticles promotes the formation of β-phase of PVDF as is evident by the evolution of the reflection peak β(200)/β(110) at $2\theta = 21^\circ$. However, in both blends addition of I.30T leads to a lower amount of the β-phase. Earlier studies on PVDF nanocomposites have already demonstrated that addition of nanoclays leads to a preferential development of the β-phase of PVDF at the expense of the α polymorph. The relative amounts of these two polymorphs depends on the processing conditions and the nature of the added nanoclay [19,21]. The additional peak observed at $2\theta = 21.3^\circ$ in Fig. 2a, is due to the crystalline polyethylene domains in EVAc.

Fig. 3 shows the DSC thermographs of the PVDF/EVAc15 and PVDF/EVAc32 series. The unfilled samples showed two distinct melting regions, due to the immiscibility of the two components at the molecular level. This is in agreement with previous studies [22] and is a direct consequence of the immiscibility of PVDF and polyethylene, while the miscibility of PVDF and VAc is thermodynamically favored. The addition of clay nanoparticles does not alter this pattern, although two important differences can be seen for both 30B filled samples; the disappearance of the double peak in the melting region of α-phase of PVDF and the development of a minor peak at higher temperatures, which is consistent with the presence of the more thermally stable β-phase of PVDF. The degree of crystallinity of EVAc15 and EVAc32 was unaffected by the addition of the clays. The crystallinity of PVDF was also virtually unaffected by the introduction of I.30T, while slightly lower values were obtained for both 30B filled blends.

The stress–strain curves of the nanocomposites are compared with the corresponding binary blends in Fig. 4. Despite the presence of the β-PVDF phase (which possesses better elongation to failure than the α-phase), the PVDF/EVAc15–30B nanocomposite exhibits almost identical mechanical performance with the unfilled sample (Fig. 4a). In contrast, the I.30T based nanocomposite exhibits significant reinforcement in terms of Young's modulus, strength and elongation at break. Nanocomposites containing 5 wt.% of clay exhibit better than 200% improvement in toughness (defined as the area under stress–strain curve).

Fig. 4b shows the tensile behavior of the PVDF/EVAc32 blend based nanocomposites. It can be seen that both nanocomposites exhibited superior mechanical performance

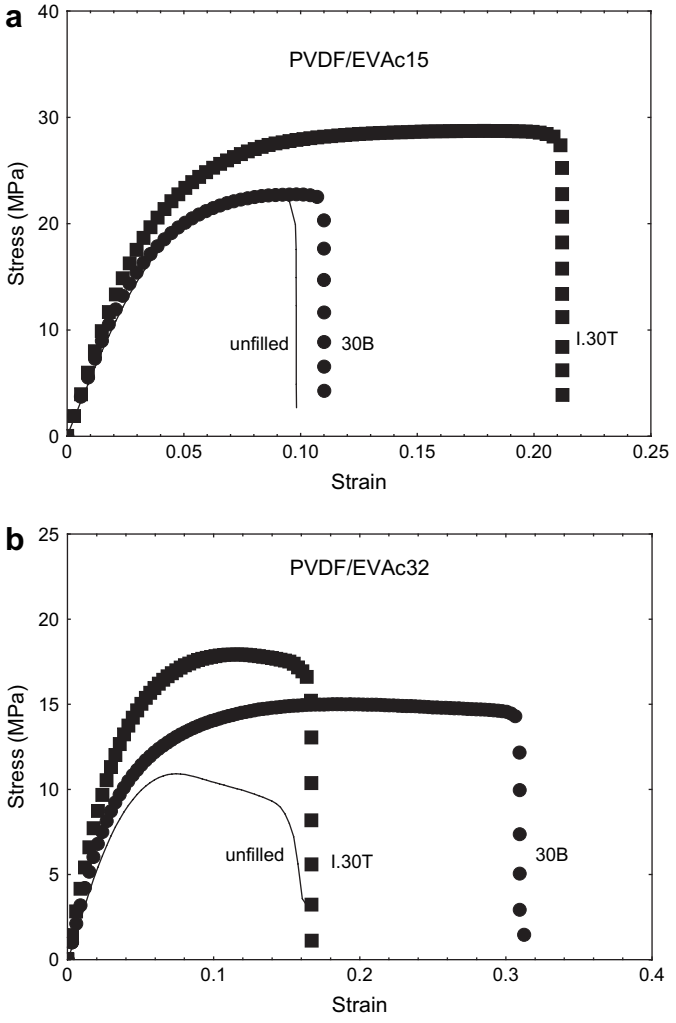

Fig. 4. Stress–strain curves of the unfilled blends (solid lines), 5 wt.% I.30T (squares), and 5 wt.% 30B (circles) nanocomposites at room temperature. Fig. 4a and b refers to PVDF/EVAc15 and PVDF/EVAc32 based nanocomposites, respectively.

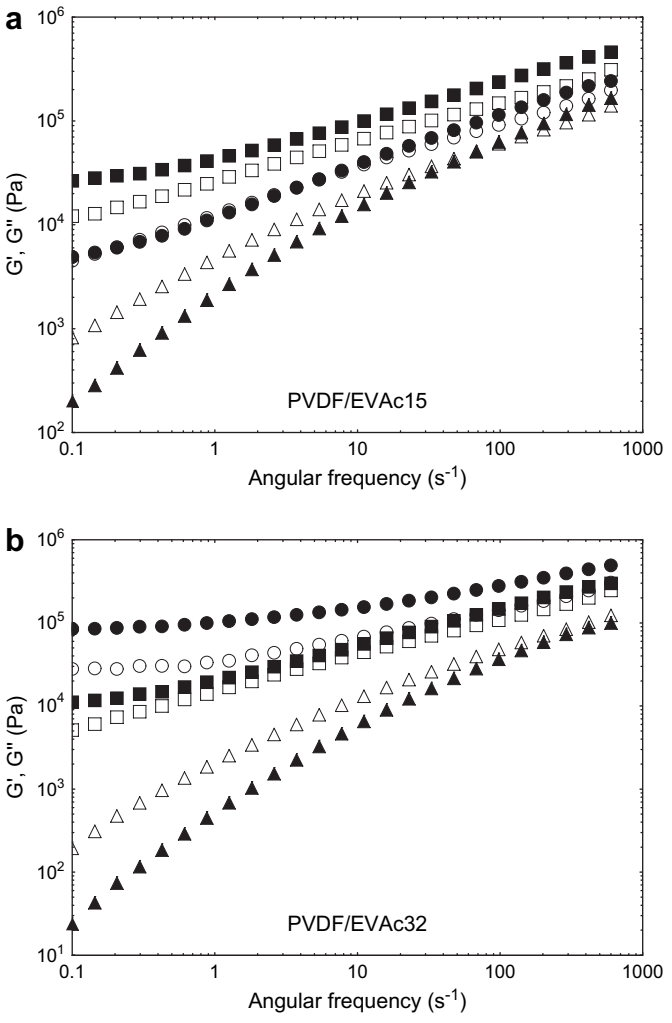

Fig. 5. Frequency dependence of storage (G') and loss (G'') moduli for the unfilled blend (triangles), the 5 wt.% I.30T (squares) and the 5 wt.% 30B nanocomposites (circles), respectively, at $T = 210\ ^{\circ}C$. Filled symbols correspond to G' and unfilled symbols to G''. Fig. 6a and b refers to PVDF/EVAc15 and PVDF/EVAc32 set of samples, respectively.

compared to the unfilled blend. The nanocomposite based on I.30T showed a considerable increase in Young's modulus, almost twice higher strength while maintaining the elongation at break. Overall, the inclusion of 5 wt.% of I.30T clay resulted in an increased mechanical toughness of about 80%. On the other hand, addition of 5 wt.% clay 30B resulted in simultaneous improvements of Young modulus, stress and elongation at break. The nanocomposite exhibits a 200% improvement in toughness. Higher Young's modulus was observed for the I.30T based nanocomposite compared to its 30B counterpart.

The dynamic moduli of the PVDF/EVAc15 and PVDF/EVAc32 nanocomposite melts measured at 210 °C as a function of frequency are shown in Fig. 5. Compared to the unfilled blends, all nanocomposites showed increased values of storage G' and loss G'' moduli within the entire frequency range studied. Moreover, the rheological response of the unfilled sample is typical of an entangled polymer melt (slopes of $G'(\omega)$ and $G''(\omega)$, 2 and 1, respectively), whereas the nanocomposite melts exhibit pseudo-solid like behavior. Pronounced deviations from this ideal melt behavior, particularly in the low frequency region is a common feature for several classes of nanocomposites [23–25] and they are considered as the signature of the evolution of physical gels. These gels can be viewed as a percolated network, in which the long-range connectivity arises from the cross-link formation (physical in nature) induced by nanofillers. For example, in Fig. 5a the crossover frequency for the unfilled blend is close to 100 rad/s, whereas that of the 30B filled sample appears at lower values. This behavior implies that in the later case the polymer chains experience increased friction forces resulting in a delayed relaxation. Even higher relaxation time can be assigned to the I.30T filled blend, indicating stronger filler-matrix interactions. An alternate approach for the pseudo-like viscoelastic response observed could be based on the jamming of nanoparticles, but this contribution should not differ significantly for samples filled with the same clay in two similar in composition matrices. The onset of jamming of nanoparticles cannot explain the reversed effects (Fig. 5) induced by the same clay in two matrices that only differ in their composition

by 4 wt.% and, therefore, this contribution was not considered as the dominant effect in the present study.

It is interesting to note that in the case of PVDF/EVAc15 based nanocomposites it is the hydrophobic I.30T that shows higher values of moduli, as opposed to the PVDF/EVAc32 based nanocomposites, where the more polar 30B clay induced stronger viscoelasticity. Moreover, a remarkable correlation between the tensile properties and the rheology of the melts can be established; the less polar PVDF/EVAc15 blend coupled with the hydrophobic I.30T clay exhibit enhanced tensile properties and also has higher viscosity, whereas the polar-rich PVDF/EVAc32 matrix coupled with the hydrophilic 30B clay shows stronger viscoelastic response and superior mechanical performance.

SEM images shown in Fig. 6 reveal the effect of addition of nanoclays on the phase morphology of the matrix. A dramatic modification of the distribution of the EVAc32 is induced by 30B (Fig. 6b, iii), whereas minor changes can be observed for the I.30T filled sample (Fig. 6b, ii). At the same time, the size of the EVAc15 domains is reduced more effectively in the case of I.30T (Fig. 6a, ii) containing samples rather than the 30B filled samples (Fig. 6a, iii). It is apparent, that the morphological characteristics and the spatial organization of the polymer domains are sensitive to the nature of the added organoclay. Favorable interactions at the molecular level (clay surface–polymer groups) are directly reflected in the mesostructural development of the nanocomposites.

The shrinkage of the suspended droplets within the continuum of the polymer blend induced by nanoclays has been probed by direct microscopy observations (SEM, TEM, AFM) in a number of studies [6–16]. Two different approaches have been proposed to explain this effect. On one hand, the kinetic approach suggests that the unequal distribution of the clay platelets between the two components of the polymer blends (as a consequence of the significant differences in the physico-chemical characteristics in a typical pair of incompatible polymers) leads to an increased viscosity of the preferentially clay enriched phase. This phase can, thus, impose stronger constrains to the diffusive motion of the other phase and by, doing so, can perturb more efficiently the coalescence of the droplets. On the other hand, the thermodynamic approach focuses on the changes of the free energy of mixing induced by the inclusion of nanoclay as a third component to the system. The selective localization of the silicate platelets along the interface of the two polymeric components can reduce the interfacial tension between the two phases, essentially promoting their mutual adhesion and improving the wetting between the two immiscible polymers of the matrix. We note that these two mechanisms can act in parallel and synergistically so that their relative contributions to the overall morphology cannot be precisely evaluated at present.

In summary we have established a relationship between the microscopic structure and the macroscopic properties in two sets of clay nanocomposites based on polymer blends

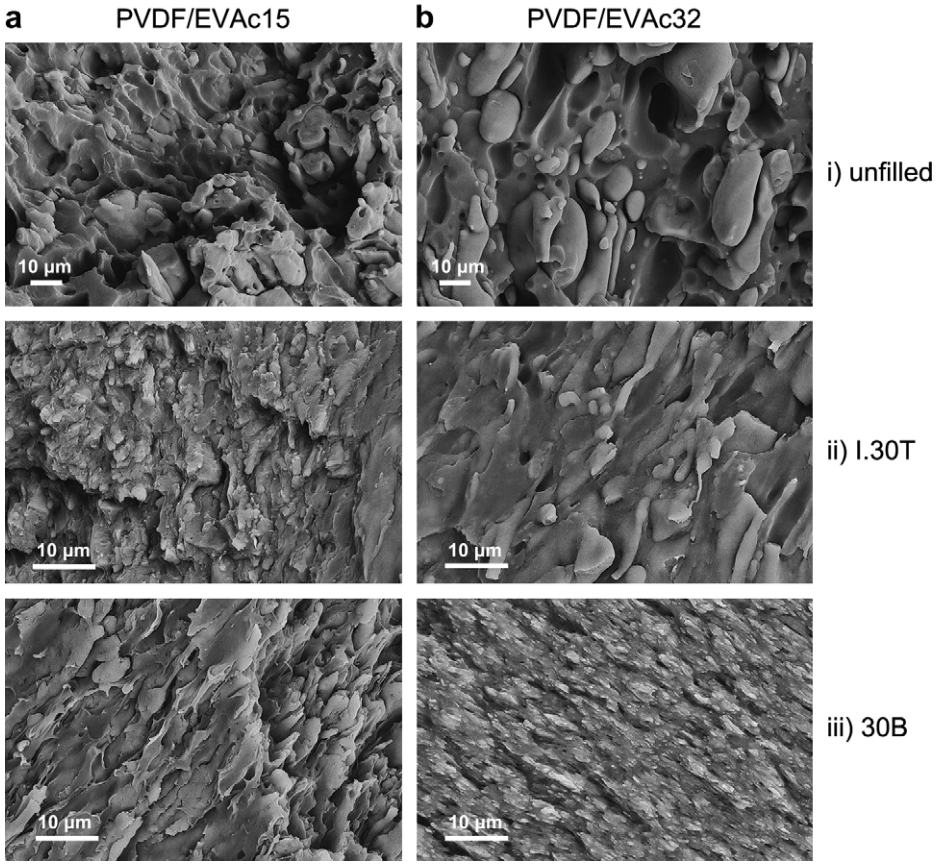

Fig. 6. SEM micrographs of (a) PVDF/EVAc15 and (b) PVDF/EVAc32 systems: (i) unfilled blends; (ii) 5 wt.% I.30T and (iii) 5 wt.% 30B nanocomposites.

comprised of poly(vinylidene fluoride) (PVDF) and ethylene–vinyl acetate copolymer (EVAc) were examined. In nanocomposites based on a polymer blend matrix with high content of polar groups (VAc) the dispersion of polar nanoclay leads to significant enhancement in toughness and a substantial increase in viscosity. However, in nanocomposite blends based on a less polar matrix (i.e. with fewer VAc groups) it is the hydrophobic organoclay that leads to higher modulus and stronger viscoelasticity. The degree of chemical affinity between the binary polymer matrix and the embedded nanoparticles has a pronounced effect on the macroscopic properties of the nanocomposites. Favorable or unfavorable thermodynamic interactions at the molecular level (clay gallery modifier–polymer groups) dictate the organization of the suspended polymer droplets in a mesoscopic scale (by determining the size of the phase separated domains), which, in turn, has a strong effect on the macroscopic characteristics of the nanocomposites. In this respect, polymer blend based nanocomposites can serve as model systems for understanding fundamental aspects of the polymer–particles interactions. Moreover, nanoclays can be used as matrix sensitive structure-directing agents that can enable precise tuning of the domain sizes and consequently control of the polymer structure and properties.

References

[1] Giannelis EP, Krishnamoorti R, Manias E. Adv Polym Sci 1999;138:107.
[2] Schmidt D, Shah D, Giannelis EP. Curr Opin Solid State Mater Sci 2002; 6:205.
[3] Ray SS, Okamoto M. Prog Polym Sci 2003;28:1539.
[4] Balazs AC, Emrick T, Russell TP. Science 2006;314:1107.
[5] Lim SK, Kim JW, Chin J, Kwon YK, Choi HJ. Chem Mater 2002;14: 1989.
[6] Voulgaris D, Petridis D. Polymer 2002;43:2213.
[7] Nanofiller modification of phase stability in PS/PMMA blends. In: Hjelm RP, Nakatani AI, Gerspacher M, Krishnamoorti R, editors. MRS proceedings, vol. 661, KK10.1.1; 2001.
[8] Gelfer MY, Song HH, Liu L, Hsiao BS, Chu B, Rafailovich M, et al. J Polym Sci Part B Polym Phys 2003;41:44.
[9] Wang Y, Zhang Q, Fu Q. Macromol Rapid Commun 2003;24:231.
[10] Ray SS, Pouliot S, Bousima M, Utracki LA. Polymer 2004;45:8403.
[11] Li Y, Shimizu H. Polymer 2004;45:7381.
[12] Khataua BB, Lee DJ, Kim H, Kim JK. Macromolecules 2004;37:2454.
[13] Yoo Y, Park C, Lee SG, Choi KY, Kim DS, Lee HJ. Macromol Chem Phys 2005;206:878.
[14] Ray SS, Bousmina M. Macromol Rapid Commun 2005;26:1639.
[15] Yurekli K, Karim A, Amis EJ, Krishnamoorti R. Macromolecules 2003; 36:7256.
[16] Yurekli K, Karim A, Amis EJ, Krishnamoorti R. Macromolecules 2004; 37:507.
[17] Shah D, Maiti P, Gunn E, Schmidt DF, Jiang DJ, Batt CA, et al. Adv Mater 2004;16:1173.
[18] Shah D, Maiti P, Jiang DD, Batt CA, Giannelis EP. Adv Mater 2005; 17:525.
[19] Pramoda KP, Mohamed A, Phang IY, Liu T. Polym Int 2005;54:226.
[20] Buckley J, Cebe P, Cherdack D, Crawford J, Ince BS, Jenkins M, et al. Polymer 2006;47:2411.
[21] Dillon DR, Tenneti KK, Li CY, Ko FK, Sics I, Hsiao BS. Polymer 2006; 47:1678.
[22] Okabe Y, Kyu T. Polymer 2004;45:8485.
[23] Krishnamoorti R, Giannelis EP. Macromolecules 1997;30:4097.
[24] Kelarakis A, Yoon K, Somani RH, Chen X, Hsiao BS, Chu B. Polymer 2005;46:11591.
[25] Krishnamoorti R, Yurekli K. Curr Opin Colloid Interface Sci 2001; 6:464.